Enhanced-Fluorescence of a Dye on DNA-assembled Gold Nano-Dimers Discriminated by Lifetime Correlation Spectroscopy

Pedro M. R. Paulo,[1] David Botequim,[1] Agnieszka Jóskowiak,[1] Sofia Martins,[2] Duarte M. F. Prazeres,[2] Peter Zijlstra [3] and Sílvia M. B. Costa [1]

[1] Centro de Química Estrutural, Instituto Superior Técnico,
Universidade de Lisboa, Av. Rovisco Pais 1, 1049-001 Lisboa, Portugal

[2] iBB – Institute for Bioengineering and Biosciences, Instituto Superior Técnico,
Universidade de Lisboa, Av. Rovisco Pais 1, 1049-001 Lisboa, Portugal

[3] Molecular Biosensing for Medical Diagnostics,
Eindhoven University of Technology, P.O. Box 513, 5600 MB, Eindhoven, The Netherlands

KEYWORDS. Surface-Enhanced Fluorescence; Gold Nanoparticle Dimers; DNA-directed self-assembly; Plasmonic nanoantennas; Fluorescence Lifetime Correlation Spectroscopy; DDA simulations.

Abstract

The surface plasmon modes of metal nanoparticles provide a way to efficiently enhance the excitation and emission from a fluorescent dye. We have employed DNA-directed assembly to prepare dimers of gold nanoparticles and used their longitudinally coupled plasmon mode to enhance the fluorescence emission of an organic red-emitting dye, Atto-655. The plasmon-enhanced fluorescence of this dye using dimers of 80 nm particles was measured at single molecule detection level. The top enhancement factors were above 1000-fold in 71% of the dimers within a total of 32 dimers measured, and, in some cases, they reached almost 4000-fold, in good agreement with model simulations. Additionally, fluorescence lifetime correlation analysis enabled the separation of enhanced from non-enhanced emission simultaneously collected in our confocal detection volume. This approach allowed us to recover a short relaxation component exclusive to enhanced emission that is attributed to the interaction of the dye with DNA in the interparticle gaps. Indeed, the frequency of enhancement events is larger than expected from the volume occupancy of the gap region, thus suggesting that interaction of the dye with DNA linkers favors the observation of emission enhancement in our dimer particles.

Introduction

In recent years an increasing number of reports have illustrated the use of plasmonic nanostructures as optical nanoantennas to modify the emission properties of fluorescent molecules or other emitters.[1-3] The phenomena described encompass emission enhancement and quenching,[4-7] tailoring of the emission spectrum or lifetimes,[8,11] and controlling emission directionality.[12,13] The role of plasmonic antennas for modifying other photophysical or photochemical processes has also been reported. For instance, plasmonic nanostructures have been employed for the manipulation of optical selection rules,[14] spatial confinement in photopolymerization,[15] enhancement of Förster energy transfer efficiency,[16] reduction of dye photobleaching[17] or improvement of energy conversion in solar cells.[18]

The strong enhancement of fluorescence emission is nevertheless one of the most promising features of plasmonic antennas. The enhancement of very weak emitters is potentially interesting for studying intrinsically fluorescent systems with low quantum yields, e.g. proteins or metal complexes, because it makes possible their detection by optical techniques without the need of labelling. On the other hand, the emission enhancement of strongly fluorescent molecules by their conjugation with metal nanoparticles can result in even brighter fluorescent objects of interest for imaging and biosensing applications. Other examples that benefit from plasmonic light confinement and emission enhancement are the detection of single molecules in concentrated solutions[19-21] and super-resolution localization fluorescence microscopy.[22-24]

The design principles to achieve emission enhancement with plasmonic antennas have been extensively studied, both theoretical and experimentally, and are well established in the literature.[1-5,25-27] The emission enhancement that is possible with a single spherical gold nanoparticle is limited to only of a few times the photon emission rate of the isolated fluorescent

molecule.[4,5] In order to obtain large fluorescence enhancements, it is necessary to employ plasmonic nanostructures that generate intense near fields. This is the case of metal nanoparticles with sharp geometrical features and of nanostructure arrays or assemblies of particles with nanometric gaps.[6,28-35] For instance, dimers of spherical gold nanoparticles are capable of enhancing fluorescence emission by two or more orders of magnitude.[21,30-34] The longitudinal coupling of the individual plasmons in dimer particles gives rise to an hybridized plasmon mode that produces an intense near field concentrated in the gap region. The field enhancement is particularly strong for dimers of gold particles of several tens of nanometer in diameter combined with gap separations of a few nanometers. Such dimer particles afford the largest emission enhancements reported up to now.[21,33,34]

The fabrication of dimer nanostructures can be accomplished by nanolithography, but precise control of gap distances down to only a few nanometers is still challenging using these methods. Alternatively, wet-chemistry synthesis and supramolecular assembly approaches give access to dimers of gold nanoparticles with narrow interparticle distances. One successful approach is the use of DNA-directed self-assembly to produce dimer nanoparticles that perform efficiently as plasmonic antennas.[10,30-33] Nevertheless, these methods generally require quite elaborate molecular arrangements of DNA (e.g. singly DNA-functionalized particles or DNA origami templates) that make the full process expensive and complex to replicate. On the other hand, the spontaneous aggregation of gold nanoparticles upon surface immobilization has also been shown to produce dimers that can be used as plasmonic antennas.[21] Although this is a very simple way to produce dimers, the process is intrinsically not selective for dimers, which then appear on the surface mixed with single particles and large aggregates.

In this contribution, we report on fluorescence enhancement of a red-emitting dye using gold nanoparticle dimers to achieve large enhancement factors. We have adapted a DNA-directed approach to assemble gold nanoparticles into dimers,[36] which is simple and does not rely on exactly one ds-DNA in the gap, while affording some control over sample's composition that is not possible with spontaneous dimer particle assembly. The performance of these dimer particles as plasmonic antennas for emission enhancement of Atto-655 fluorescent dye was investigated by single molecule fluorescence microscopy. The dimers of gold particles having a diameter of 80 nm afforded top emission enhancements of almost 4000-fold, which are comparable to the largest enhancement factors reported so far.[21,33] We have also introduced a fluorescence lifetime correlation analysis in order to separate the dimer enhanced from non-enhanced emission of dye molecules within the confocal detection volume.

Experimental

Materials

Gold nanoparticles with sizes of 80 nm and 40 nm, stabilized by a citrate coating, were acquired from Nanopartz Inc. as aqueous suspensions with an optical density of 1 (product no. A11-80 and A11-40). DNA oligonucleotides purified by HPLC were purchased from STAB Vida (Monte da Caparica, Portugal). DNA strands with (n + 10) nucleotides and having the general sequence 5'-SH-$A_{10}N_n$-3' were used. Two oligonucleotides were designed for *n* equal to 15, 30 or 60, in such a way as to form hybrids by base pairing of the N_{15}, N_{30} and N_{60} sequences (see diagram D1 in the SI). Tris base (Eurobio, molecular biology grade), boric acid (Fisher Chemical, assay 100%) and EDTA (TCI Europe, 98%) were used to prepare TBE buffer. Sodium citrate tribasic

dihydrate (Sigma-Aldrich, ≥ 99.5%) and hydrochloric acid (Sigma-Aldrich, 37%) were used to prepare citrate buffer. Ultrapure water was obtained with a Milli-Q purification system (Merck-Millipore). Agarose with electrophoresis purity degree was purchased from NZYTech. Polyethylenimine, branched polymer with an average Mw ~25,000 was purchased from Aldrich.

Equipment

Extinction spectra were measured in an UV/Vis spectrophotometer from PerkinElmer, model Lambda 35. TEM characterization was performed on a HITACHI H-8100 electron microscope operating at 200 kV. Glass surfaces were cleaned using an UV/Ozone chamber model PSD-UV3 from Novascan. Single-molecule fluorescence experiments were performed on a confocal fluorescence lifetime microscope, MicroTime 200 (PicoQuant GmbH). The microscope setup details were previously described.[37] The single-particle spectra were obtained by means of a low light level spectrometer, QEPro (Ocean Optics), that was fiber coupled to the confocal microscope. Data acquisition and preliminary analysis were performed on SymPhoTime software (PicoQuant GmbH). This program was also used to carry out data analysis by Fluorescence Lifetime Correlation Spectroscopy (FLCS).[38,39]

Preparation of Gold Nanoparticle Dimers

The first step was the hybridization of the thiolated DNA oligonucleotides to form a DNA linker with two thiol moieties, one at each end of the double strand (see diagram D1 in the SI). Then, the double-stranded DNA linkers were used to assemble gold nanoparticles into dimers and larger aggregates in a similar approach to that described in Ref. 36. The concentration of DNA used was determined from the theoretical maximum number of thiolated chains per particle, i.e. approx. 1400 and 430 chains for gold particles with 80 and 40 nm, respectively.[40] The DNA

hybridization was performed by mixing the complementary sequences (8 μL each) with TBE buffer (0.5×, 4 μL) containing added NaCl salt (200 mM). The mixture was heated up to 80 ºC for 15 min, then cooled down to room temperature, and left to rest overnight. The gold nanoparticles were concentrated by centrifugation from a volume of ~1000 μL of the solution supplied (OD ~1) and collecting a volume of 26 μL from the pellet. This volume of particles was added to the DNA hybridization mixture under vigorous stirring and left to pre-incubate for 30 mins. Afterwards, a citrate buffer solution was added to the hybridization mixture. The citrate buffer solution was prepared according to the low pH protocol of Zhang et al.[41] The citrate buffer was added gradually by mixing 2 μL of buffer solution each time, followed by stirring and resting for 10 min before the next addition, up to a total of 4 addition steps. The final incubation time was 60 min. The reaction was halted by washing off the excess of DNA by centrifugation and replacing the supernatant with 0.5× TBE buffer.

Gel electrophoresis was used to separate single particles from dimers and higher aggregates. The concentrations of agarose gels used were 0.7% and 1.5% for particles sized 80 and 40 nm, respectively. All gels were run at 120 V in 0.5× TBE buffer. Two red bands were typically obtained after 30 min. These particle-containing agarose fractions were cut from the gel and placed in a microtube filled with approx. 0.5 mL of 0.5× TBE buffer. The particles were allowed to diffuse from the gel pieces for at least one week. Samples containing the extracted gold nanoparticles were characterized by TEM, showing that the fraction extracted from the slowest migrating band contained mostly dimers.

Surface Immobilization of Gold Nanoparticle Dimers

Round glass coverslips were cleaned by sonication in aqueous solution of RBS50 detergent 5% (w/v) during 30 mins, followed by another sonication in absolute ethanol, and rinsing with water after each step. The dried coverslips were then irradiated for 2 hrs in a UV/ozone chamber. Before particle immobilization, the glass surface was coated with polyethyleneimine.[42] First, the coverslips were dipped in a cold piranha bath for 10 mins to improve the surface wettability, then rinsed copiously with water and dried. The polymer coating was deposited by covering the surface with an aqueous solution of polyethyleneimine 0.2% (w/v) during 20 mins, then rinsing with water and nitrogen blow drying. The gold nanoparticle dimers were immobilized by spin coating 10 μL from a dilute (sub-nM) aqueous solution of these particles.

DDA simulations

Simulations of discrete dipole approximation (DDA) were performed in order to theoretically estimate the emission enhancement using dimers of gold nanoparticles. The free software implementation A-DDA was used for running these simulations.[43] The model dimers were defined by discretization of the particle volume as an array of cubic volume elements with a side length of 0.5 nm. The dielectric function of each element is the same of bulk gold, and the values reported by Johnson and Christy were used,[44] but scaled by the dielectric constant of water to include the refractive index of the surrounding environment. The simulated particle diameter was 80 nm and the interparticle gap distance was varied between 2 and 10 nm. The extinction spectrum of dimer nanoparticles was reconstructed from the extinction cross-section calculated for a series of incident wavelengths between 500 and 900 nm. The polarization of the incident plane-wave was selected to be either parallel or perpendicular to the interparticle axis, therefore

exciting respectively the longitudinal and transversal hybridized plasmon modes in the dimer particle.

The estimation of fluorescence enhancement using DDA calculations has been previously described.[28,35] The overall emission enhancement (F/F^0) can be estimated from DDA calculations as the product of the excitation rate enhancement (E_{exc}) and the emission quantum-yield of the dye modified by the dimer nanoparticle (ϕ/ϕ^0). The excitation rate enhancement is obtained from $E_{\text{exc}} = |\boldsymbol{E}|^2/|\boldsymbol{E_0}|^2$, which is the near field enhancement at the incident wavelength (639 nm) in the position assumed for the dye molecule. The near-field intensity maps around the gold nanoparticles were calculated using the subroutine implemented in the A-DDA software package.[45] The calculation of the modified quantum-yield requires the estimation of the enhanced radiative and non-radiative decay rates. The theoretical formalism described by D'Agostino et al. was used for this purpose (see SI).[46]

Results and Discussion

The dimers of gold nanoparticles used in fluorescence enhancement experiments were produced by bridging two nanoparticles with a DNA-based linker formed by hybridizing two thiolated oligonucleotides. These short linkers contain a central, double-stranded region of less than 60 base pairs and overhanging single strand segments with 10 nucleotides. These short linkers yielded dimers with interparticle gaps of a few nanometers that can be observed in the TEM images (Fig. 1A, B). The gap distances are shorter than the length of the double-stranded region because of the single strand segments on both ends of the DNA linker. The fraction of dimer particles obtained after purification by gel electrophoresis, as observed from TEM images, was

on average 68%, while single particles represent 23% of analysed samples. Single particles are present as smear in the gel and end up as a contamination in the dimer sample when extracted from the respective gel band (inset of Fig. 1C). Gold nanoparticles that are only citrate-stabilized show a gel without any bands, only a smear is visible, which emphasizes the role of thiolated DNA linkers in particle assembly (Fig. S1 of the SI).

The optical extinction spectrum of dimer particles features two surface plasmon bands instead of the single band that is characteristic of single gold nanoparticles (Fig. 1C). This occurs because of plasmon coupling between the individual modes in neighbouring particles of the dimer gives rise to two optically active hybridized plasmon modes.[47] The surface plasmon band appearing at longer wavelengths corresponds to the bonding mode, and it generates strong local fields across the interparticle gap that are interesting for fluorescence enhancement. The resonance wavelength of the longitudinal plasmon mode depends strongly on the gap separation. For instance, at shorter gap distances the plasmon coupling is stronger and this energy stabilizing interaction induces a shift of the longitudinal surface plasmon band toward longer wavelengths. This effect is illustrated in Figure 1D that shows the calculated extinction spectra for dimers of gold particles of 80 nm simulated with gap distances of 2, 3 and 4 nm – red, orange and green curves, respectively. Using this plasmon ruler obtained from simulated spectra (inset of Fig. 1D), we estimate from the experimental spectrum of our dimer sample that the average interparticle distance is around 2 to 3 nm.

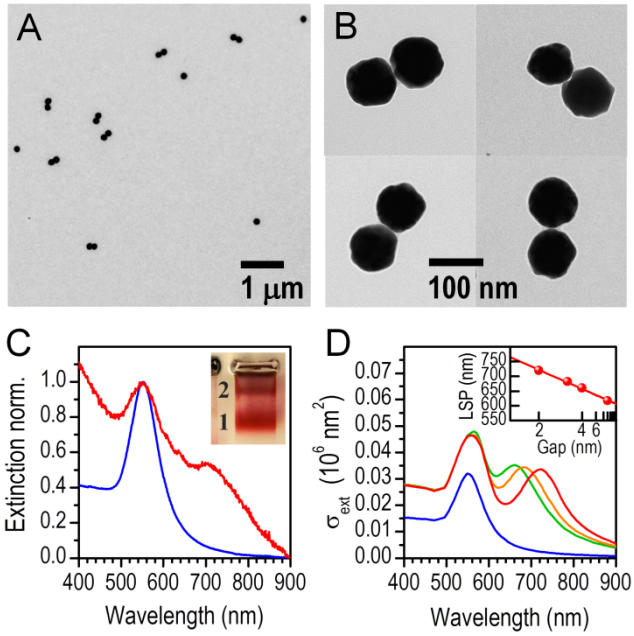

Figure 1. A) Electron microscopy images of dimers of gold nanoparticles with a diameter of 80 nm assembled by a DNA linker with a 60-bp double-stranded region. B) Magnification of TEM images of four selected examples of dimer nanoparticles. C) Extinction spectrum of dimers of gold nanoparticles (red curve) extracted from the gel band no. 2; and that of gold nanoparticles functionalized with DNA, but not-dimerized (blue curve), separated from gel band no. 1– the inset shows a photograph of the gel with bands indicated. D) Calculated extinction spectra from DDA simulations of a single gold nanoparticle of 80 nm (blue curve) and that of dimer nanoparticles with a gap separation of 2, 3 and 4 nm (red, orange and green curves, respectively) – the inset shows the peak wavelength of the longitudinal surface plasmon band (LSP), as a function of the gap separation considered in DDA simulations.

The dimer particles were further characterized by their optical spectrum measured at the single-particle level. For this purpose, dimer samples were immobilized onto glass coverslips at

low surface density. The optical microscopy images show diffraction-limited spots with a narrow dispersion of emission intensity (Fig. 2A and B). The photoluminescence spectrum was collected from several of these spots on each image. The spectrum of dimer particles typically features two bands: one more intense at around 550 nm followed by another band or shoulder at longer wavelengths (Fig. 2C). It is clearly different from the spectrum of single particles that show only one band at 550 nm with a Lorentzian lineshape – as exemplified in spectrum no. 6 of Fig. 2C. Also, the emission intensity from dimer particles is approximately twice that of single particles and, in addition, the emission from single particles is non-polarized, while the dimers emission displays polarization in the sample plane (Fig. S2 of the SI). These features allow to easily distinguish the emission of individual dimers from that of a minor fraction of single particles that is always present even after purification by gel electrophoresis.

The emission spectrum of dimer particles changes slightly from particle to particle within each sample. In fact, the flexible ends of the DNA oligonucleotide linkers allow for some variation in the gap distance between paired particles, which strongly affects the longitudinal surface plasmon band of the dimer spectrum. This variation in the gap distance was firstly noticed in the TEM images of dimer samples (Fig. S3 of the SI). Another contribution to heterogeneity in the emission spectrum of individual dimers arises from deviations from the spherical shape of the gold nanoparticles. Nevertheless, we have used the plasmon ruler shown in the inset of Figure 1D to approximately infer about the interparticle gap distance in individual dimer particles from their single particle spectra.

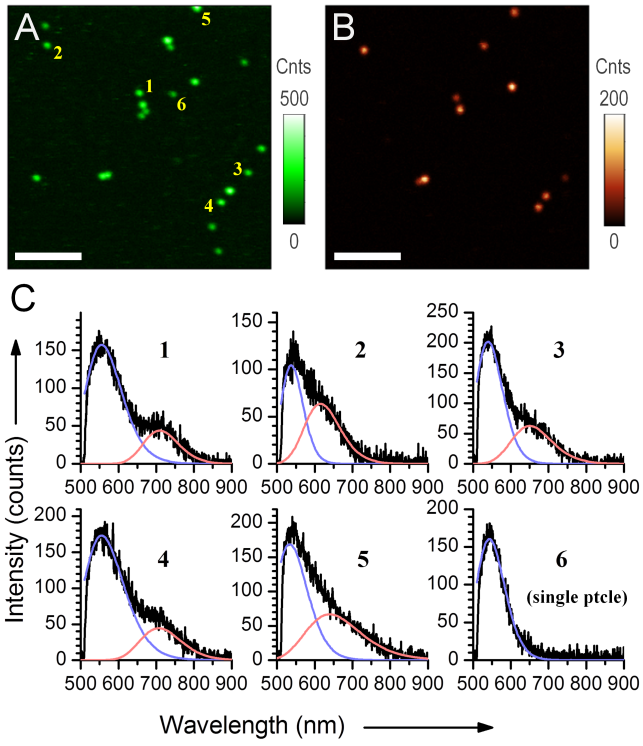

Figure 2. A) Optical microscopy image of dimer nanoparticles obtained with excitation at 482 nm (~50 kW/cm^2) and detection with a longpass filter above 510 nm. Each spot on the image is a single dimer nanoparticle or an individual particle of size 80 nm – the scale bar is 5 μm. B) The same area scan as shown in image A obtained with excitation at 639 nm (~4 kW/cm^2) and detection with a bandpass filter centred at 695 nm with a transmission window of 55 nm. C) Photoluminescence spectrum of single dimer particles identified as spots 1 to 5 in image A, and one example of an individual gold nanoparticle labelled no. 6.

The measurement of fluorescence enhancement in the emission of Atto-655 dye was performed by collecting light from a spot where an individual dimer was found. For this purpose, the dimer sample was immersed in a nanomolar solution of Atto-655 molecules, which during

the measurement diffuse and explore the space surrounding the individual dimer (Fig. 3A). The interparticle gap is the hot-spot for fluorescence enhancement because of the large local field created there by the bonding plasmon mode. The broad spectral distribution of this plasmon mode, ranging from 600 to 800 nm, is suitable for fluorescence enhancement of a wide range of red-emitting dyes. The most favorable situation occurs when the dye's emission is slightly red-shifted relatively to the plasmon resonance frequency, in order to minimize energy dissipation by the particle's absorption. The emission of Atto-655 is well matched with the longitudinal mode in dimers' spectra (Fig. 3B) and, for this reason, this dye was chosen to illustrate fluorescence enhancement.

The enhancement effect was measured by using laser excitation at 639 nm, which addresses both the dye's absorption and the longitudinal plasmon band of the dimer nanoparticles. At this excitation wavelength, the photoluminescence images show only spots from dimer particles (Fig. 2B), and their relative intensity is determined by the overlap between the dimer's spectrum and the emission filter range (Fig. 3B). The signal collected from the dimer nanoparticles in the absence of Atto-655 is steady over long observation times (orange trace in Fig. 3C). When the dye is added to the solution, the time traces begin to show strong emission bursts (red trace in Fig. 3C) that are several orders of magnitude more intense than the dimers' background signal. The emission of Atto-655 molecules in solution was also collected from a surface region free of dimer nanoparticles (grey trace in Fig. 3C). In this case, the background emission from Atto-655 within the confocal detection volume of the microscope is detected, but without any events of intense fluorescence emission.

Therefore, strong fluorescence bursts are only detected from spots where dimers are immobilized and when Atto-655 molecules are present in solution. These bursts are attributed to

the exploration of hot-spot regions on the surface of dimer nanoparticles by Atto-655 molecules diffusing in solution and transiently interacting with the DNA. The gap region is a very small volume, in the order of zeptoliter, when compared to the confocal detection volume which is around four femtoliters. For the typical concentrations of Atto-655 used in our measurements, the dye's occupation number in the confocal detection volume varies between 1 and 10, and thus, the occupation probability of the gap region is several orders of magnitude lower, as further discussed below. For this reason, the probability of multiple occupancy of the gap region is negligible, and each burst is ascribed to the exploration of the interparticle gap by only one dye molecule. The strong fluorescence bursts experimentally observed then result from single Atto-655 molecules exploring the interparticle gap region.

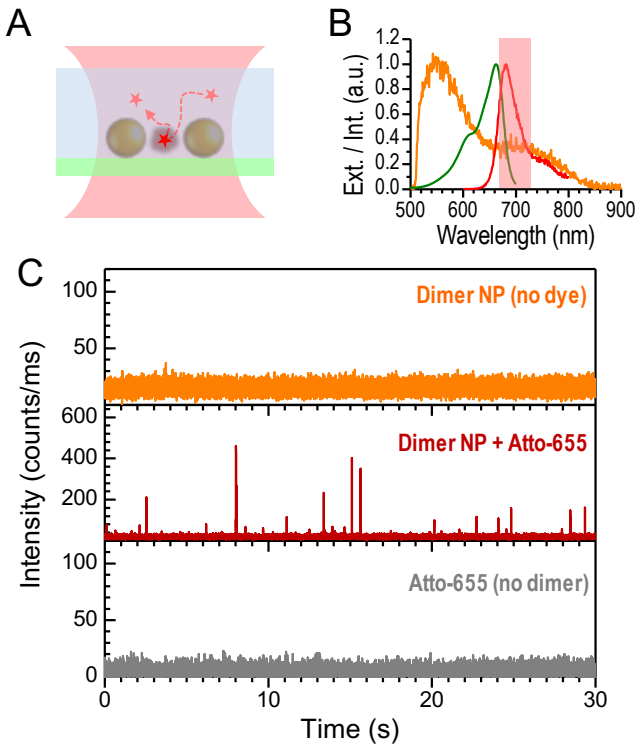

Figure 3. A) Scheme of the fluorescence enhancement experiment showing a single Atto-655 dye molecule (red star) diffusing through the gap (hot-spot) of a dimer nanoparticle. B)

Photoluminescence spectrum of an individual dimer nanoparticle (orange curve) overlapped with the absorption and emission spectra of Atto-655 dye (green and red curves, respectively), and the detection range of the bandpass emission filter (light pink rectangle). C) Emission intensity time traces measured from the spot of an individual dimer nanoparticle in the absence of Atto-655 dye in solution (top, orange curve); emission time trace from the same spot as before, but in the presence of Atto-655 dye in nanomolar concentration (middle, red curve); emission time trace from a region of the surface without any particle, but in the presence of Atto-655 dye in the same concentration as previous (bottom, grey curve).

The duration and intensity of each fluorescence burst is closely related to the trajectory of the Atto-655 molecule as it diffuses across the interparticle gap. In this region, the plasmon's near field changes rapidly. Likewise, the enhancement of the dye's excitation and emission varies as the dye molecule changes its position in the gap. The spatial dependence of the emission enhancement effect together with the randomness of the dye's trajectory explains the intensity variations observed from burst to burst within each time trace collected for several dimers. In order to characterize the enhancement effect, we will focus our discussion on the most intense event of each time trace. Some examples of intense bursts observed for dimers of 80 nm gold particles are presented in Figure 4A-D. We assume that if the observation time is long enough, then the most intense event should correspond to the molecular trajectory through the region of largest fluorescence enhancement. The strongest burst in each trace was used to calculate the top enhancement factor, which is the ratio between enhanced and non-enhanced emission for that event. The top enhancement factor is then calculated from the maximum burst intensity corrected for the background signal and normalized to the average intensity of a non-

enhanced Atto-655 dye. The latter was determined to be 0.35 counts/ms for the same conditions of the enhancement experiment (Fig. S4 of the SI).

We have found that dimers of gold particles with 40 nm give maximum enhancement factors between 500 and 1000-fold (open symbols in Fig. 4E). On the other hand, dimers of 80 nm particles are able to enhance the emission of Atto-655 by more than a 1000-fold, and in several examples, the top enhancements reach almost 4000-fold (closed symbols in Fig. 4E). As expected, the emission enhancement increases with the dimer particle size, because the radiation efficiency of the plasmon also increases. Surprisingly, a fraction of 16% of the dimers of 80 nm particles do not show any enhancement events in the sampled time interval of 60 s. This is tentatively attributed to an obstruction of dimer gaps with an excess of DNA linkers that prevents the dye to access the hot-spot region. However, about 71% out from a total of 32 dimers analysed show events with top enhancements above 1000-fold, and out of these about 16% are above 3000-fold.

The top enhancement factors reported here match up the largest known values from the literature for plasmonic emission enhancement of single-molecule fluorescence. Other examples of enhancements larger than 1000-fold have been obtained with gold nano-bowtie or nanorod antennas.[6,7,28] Recently, enhancement factors of 5000-fold on the emission of Atto-655 were reported with a system that uses complex nanostructures of DNA origami to assemble dimers of gold nanoparticles.[33] Another work reported on fluorescence enhancement using dimers spontaneously assembled by particle aggregation upon surface immobilization, which resulted in enhancement factors of more than 1000-fold.[21] Dimer nanoantennas produced by nanolithography showed enhancements of 15000-fold for the weakly fluorescent crystal violet, while the enhancement reported for the fluorescent dye Alexa Fluor 647 was around 1500-fold.[34]

In comparison, the dimer antennas used in this work deliver comparable or better enhancement factors, while allowing for control over sample composition which is not possible with spontaneous aggregation, but using a DNA-directed assembly approach that is considerably more simple and affordable than those based on DNA origami.

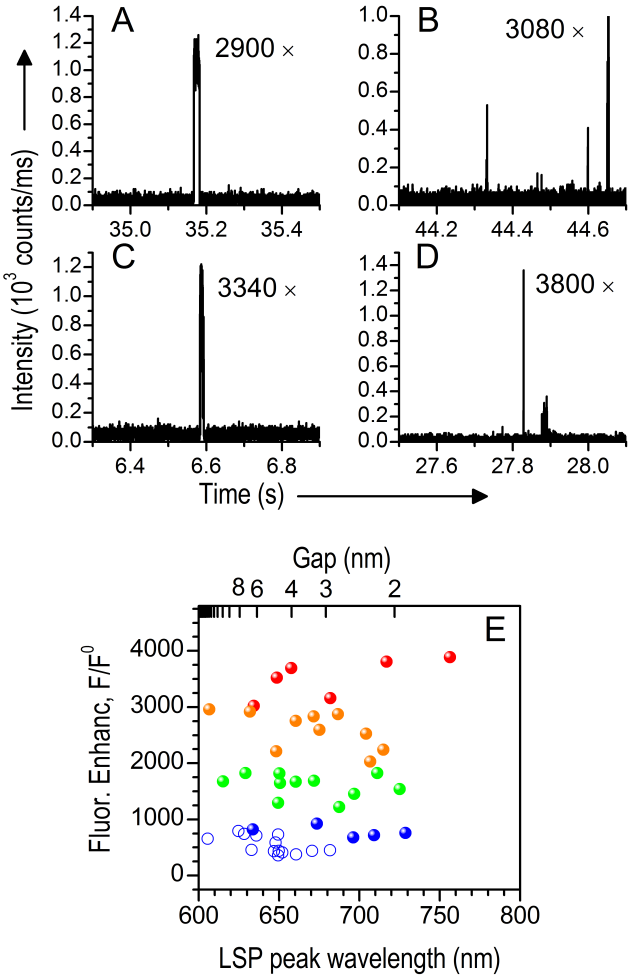

Figure 4. A-D) Examples of intense fluorescence bursts from Atto-655 emission enhanced by dimers of gold nanoparticles – the emission enhancement factor corresponding to each burst is indicated inside the figure. E) Top emission enhancement factors for single-molecule fluorescence of Atto-655 dye plotted against the LSP peak wavelength of the individual dimer nanoparticles used for fluorescence enhancement. Each symbol represents a measurement on a

different dimer nanoparticle. The symbols are color coded according to the enhancement factor: blue, < 1000; green, 1000 - 2000; orange, 2000 - 3000; red, > 3000. The open and closed symbols show enhancement factors obtained for dimers of 40 nm and 80 nm particles, respectively.

The single-particle spectrum is known for each dimer used for fluorescence enhancement, which allows us to plot the top enhancement factor relative to the peak wavelength of the longitudinal surface plasmon band (Fig. 4E). This plot does not show any particular trend between these two experimental observables, in contrast with other plasmonic nanoparticles used for fluorescence enhancement, such as single gold nanorods.[28] A plausible explanation for the lack of correlation between top enhancements and the LSP peak wavelength of dimer particles is the molecular congestion of gaps with DNA linkers that, by randomly occupying the interparticle volume, may limit or obstruct the dye's access to the central region of the hot-spot. In ref. 21, it was demonstrated that, upon attaching bulky thiolated-PEG chains onto the surface of dimer particles, the respective enhancement factors decrease, in agreement with an exclusion effect of the dye from the dimer hot-spot due to molecular crowding of the interparticle gap. Even though, in our case, the dimers are extensively coated with DNA, these linkers do not seem to have such a detrimental effect, and large enhancement factors above 1000-fold can be measured in 71% of the dimers analysed. Actually, we hypothesize that the DNA linkers may even favor the interaction between Atto-655 dye and the dimers' hot-spot, as supported by a simple argument based on the hot-spot volume and its expected occupancy. For this purpose, we have first determined from DDA near field simulations that the decay length of the plasmon field is around 10 nm in a direction perpendicular to the interparticle axis (for a dimer of 80 nm particles with a

gap of 10 nm). Assuming that the hot-spot is approximately cylindrical with radius and height of 10 nm × 10 nm gives a volume of 3.1 zL, which for an average dye concentration around 4 nM gives an occupancy of 7.6×10^{-6} molecules in the hot-spot. During an observation time of 60 s, the calculated occupancy would correspond to one molecule being present in the hot-spot for about 450 μs, which would result on average in only a few enhanced-emission bursts per time trace using a binning of 100 μs, as used in data analysis. The frequency of burst events observed is much higher, ranging from 20 events up to several hundred per trace (Fig. S5 of the SI). Thus, we hypothesize that the dye's interaction with the DNA somehow favors the occupancy of the hot-spot and the observation of fluorescence enhancement from our dimer particles.

We have performed model simulations of gold nanoparticle dimers to compare theoretically predicted fluorescence enhancements with our experimental results. The model dimers were defined for a particle size of 80 nm and the interparticle gap was varied between 2 and 10 nm, i.e. in the range of those experimentally inferred from optical spectra. The gap region is where the near field enhancement is mostly concentrated (Fig. 5A). Even for a gap separation of 10 nm, the near field enhancement corresponds to an intensity increase of almost 1000-fold along the interparticle axis, but it decays within approx. 10 nm. We have assumed three fixed positions of the dye in the gap to evaluate how the fluorescence enhancement changes with the position (right side of Fig. 5A). It also makes it possible to discuss how the maximum enhancement effect would be limited if access to the central regions of the hot-spot is restricted by molecular congestion of DNA linkers. The enhancement of fluorescence emission results from the combined changes in the excitation, radiative and non-radiative decay rates of the dye induced by interaction with the nanoparticle antenna. The enhancement factor of excitation rate (E_{exc}) and fluorescence quantum yield (ϕ/ϕ^0) were calculated separately, as presented in the SI.

Here, we will focus the discussion on the overall emission enhancement, i.e. $(F/F^0)_{\text{calc}} = E_{\text{exc}} \times (\phi/\phi^0)$, and on the enhanced fluorescence lifetime, i.e. $\tau = 1/(K_{\text{r}} + K_{\text{nr}})$.

The overall emission enhancements calculated for the central position of the gap yielded values ranging from 1000 to 10000-fold increase in the dye's emission (Fig. 5B). This result compares well with our experimental top enhancement factors which range from 1000 to almost 4000-fold. The comparison is made on the basis of the top enhancement values experimentally measured assuming that these correspond to the dye being close to gap's centre, where the largest enhancements are expected. Actually, the absolute maximum is probably at some position along the interparticle axis shifted away from the centre, where there is an optimal radiative over non-radiative decay rate enhancements.[32] On the other hand, the intensity distribution of each fluorescence burst experimentally measured is affected by the trajectory and residence time of the dye in the gap. The position dependence of the enhancement effect can be evaluated from the values of $(F/F^0)_{\text{calc}}$ for positions away from the gap centre (semi-filled and open symbols in Fig. 5B). The enhancement effect decays by orders of magnitude over a few tens of nanometers, as it closely follows a similar distance dependence of the excitation rate enhancement. As previously hypothesized, the lack of correlation between top enhancements and the LSP peak wavelength of dimer particles may be explained by molecular hindrance of DNA linkers that limits the dye's access to the central region of the hot-spot. The strong spatial dependence of the overall emission enhancement, as seen in our calculations, suggests that this is a plausible explanation.

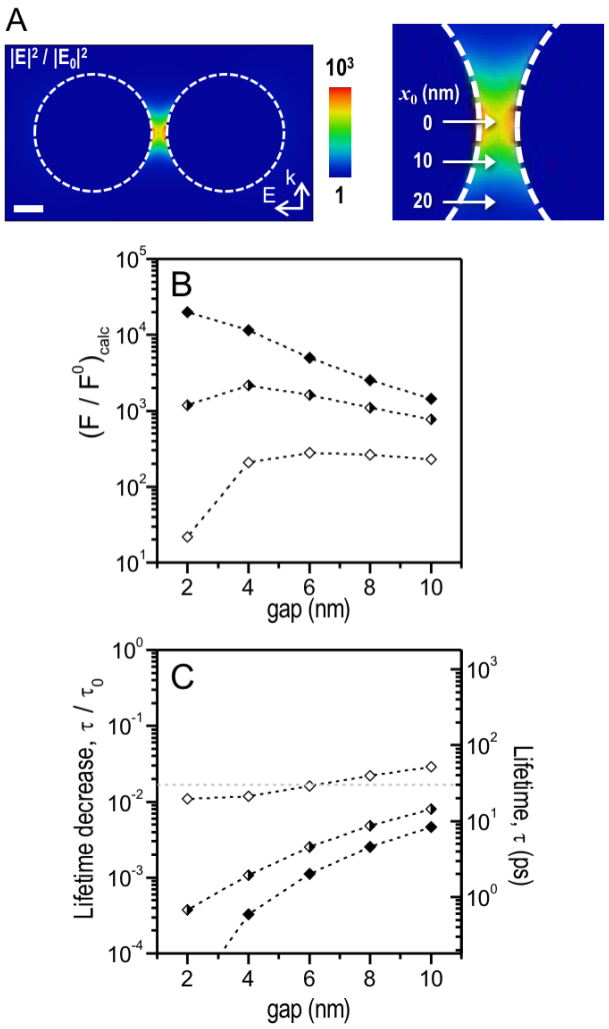

Figure 5. A) Near field maps calculated from DDA simulations of a dimer of gold nanoparticles with a size of 80 nm and a gap separation of 10 nm for an incident wavelength of 639 nm polarized across the interparticle axis – the scale bar is 20 nm. The near field map on the right shows a magnification of the interparticle gap where the positions considered for the point-like dipole of the emitting dye molecule were fixed – the number shown is the displacement in nm away from the interparticle axis. B) Enhancement factor calculated for the overall fluorescence emission $(F/F^0)_{\text{calc}}$ for the interaction of Atto-655 dye with a dimer of gold nanoparticles of size 80 nm at different gap separations – closed symbols correspond to a dye molecule

positioned at the interparticle joining axis, semi-filled and open symbols are for a position 10 and 20 nm away from the axis, respectively. C) Fluorescence lifetime decrease (τ/τ_0) calculated for the same conditions described before, where τ_0 is the decay time of Atto-655 in water (1.8 ns).

The interparticle distance has a pronounced effect in the longitudinal LSP peak wavelength, as well as in the fluorescence enhancement although in two opposite ways. Short interparticle distances induce larger near fields in the gap, which favor the dye's excitation and radiative decay rate enhancements, but the close proximity of the metal surface also favors the non-radiative decay through energy transfer and ohmic losses. The interplay between these opposing factors reduces the variation of emission enhancement with the LSP peak wavelength (or conversely, the gap distance) in dimer particles. On the other hand, the effect on the fluorescence lifetime from the acceleration of radiative and non-radiative decay rates is always characterized by a pronounced lifetime decrease (Fig. 5C). The predicted decay rates in the hot-spot region are in the ps and sub-ps timescales, which is below the time resolution of our setup (grey dashed line). Indeed, the fluorescence decays retrieved from strong burst events show a decay profile that approximately coincides with the instrument response function (Fig. S6 of the SI).

The fluorescence emission time traces contain detected photons from both enhanced and non-enhanced dye molecules within the confocal detection volume (Fig. 6). In order to separate these two contributions, we have used the information about fluorescence lifetime to analyse our results by fluorescence lifetime correlation spectroscopy (FLCS).[38,39] Fluorescence enhancement by plasmonic antennas is characterized by the acceleration of excited-state decay rates, and thus

the emission from enhanced dye molecules can be distinguished from that of non-enhanced molecules by its short decay time. The fluorescence decays recorded simultaneously with each emission trace shows multi-exponential decay profiles, which can be decomposed in short and long decay components, as shown in Figure 6B (red and blue curves, respectively). The short decay components are attributed to the enhanced decay rates of the dye together with some background signal from the dimer particle. It can be described by two exponential components with average decay times of 70 ps (84.5%) and 1.08 ns (3.5%). The long lifetime of 2.44 ns is similar to the lifetime of Atto-655 in aqueous solution (1.8 ns), although it is slightly longer probably due to adsorption onto the polymer-glass substrate. The FLCS analysis uses the decay components previously defined from decay analysis to build mathematical filters (Fig. 6C), which are then used to weigh the detected photons in order to retrieve separate correlation functions for each decay component (Fig. 6D). In this work, the FLCS analysis was used to distinguish between the correlation function of photons from enhanced dye molecules, which are associated with short decay times, from that of non-enhanced molecules (red and blue curves in Fig. 6D, respectively).

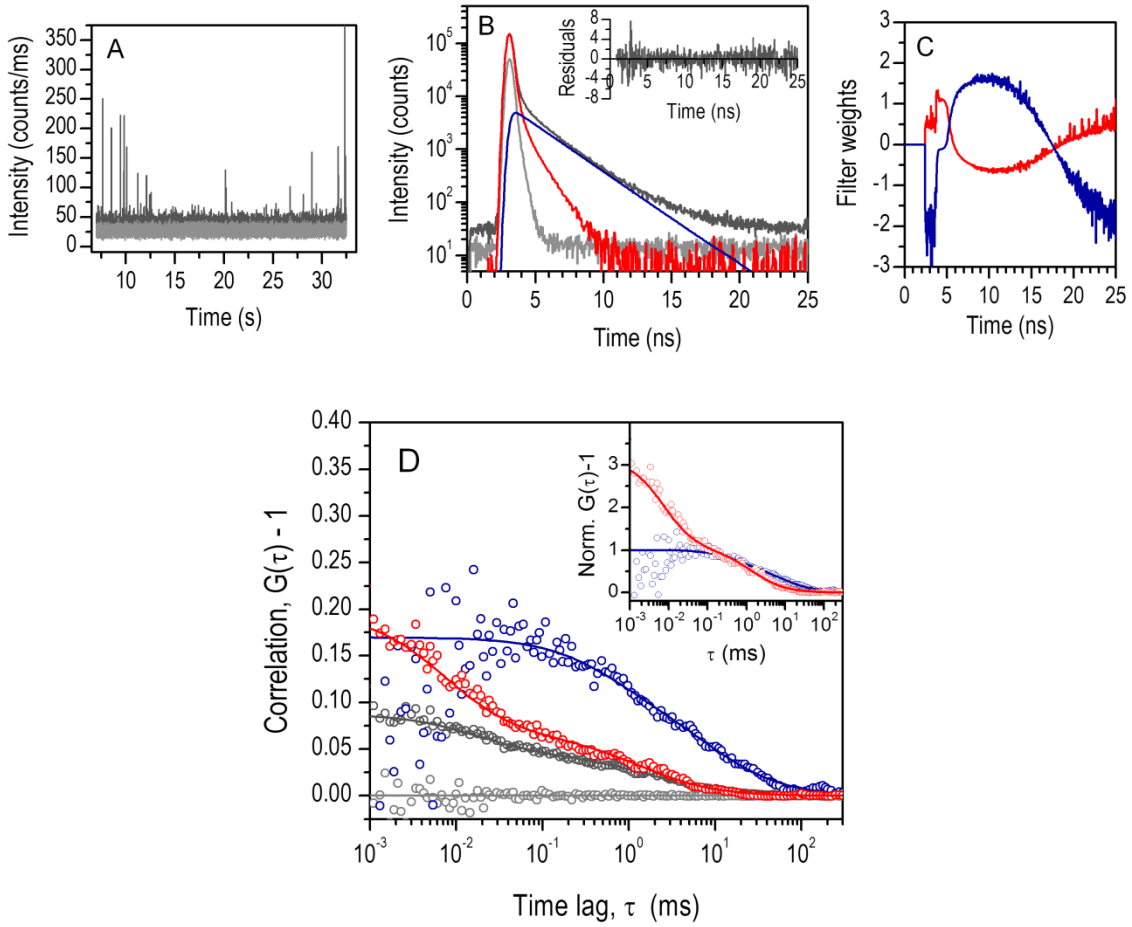

Figure 6. A) Emission intensity time trace showing intense fluorescence bursts from Atto-655 enhanced emission (dark grey) and background signal from the dimer particle alone (light grey). B) Fluorescence decay of the same emission trace (dark grey) decomposed into short and long decay components shown as red and blue curves, respectively (IRF is depicted in light grey, and the inset shows the weighed-residuals from a tri-exponential fit). C) Filter weights obtained by FLCS analysis based on the short and long decay components defined to separate the enhanced and non-enhanced emission (red and blue curves, respectively). D) Correlation curve of enhanced and non-enhanced emission (red and blue curves, respectively) obtained by FLCS

analysis, and non-filtered correlation curve of the emission trace (dark grey) and of the background signal (light grey), as shown in (A).

The main difference between the correlation function of enhanced and non-enhanced emission is that the first one shows an additional decay at short times that is not present in the latter. We have confirmed this trend by performing the FLCS analysis of other emission traces showing substantial enhancement effects (Fig. S7 of the SI). We have fitted the correlation functions with the commonly used free-diffusion model, which afforded reasonable fits using two to three diffusion terms. The free-diffusion model is used here just to extract relaxation times, which are then compared to calculated diffusion times, in order to discuss the possible origin of the several decay components observed in the correlation function. As it will later become obvious, the free-diffusion picture is not adequate to explain our results. The fast decay component that is only present in the correlation function of enhanced emission has an average relaxation time of 20 μs, and it can be associated with the short and very intense fluorescence bursts observed in emission traces. Assuming that these events correspond to dye molecules crossing the hot-spot in the gap region, the expected free-diffusion time would be in the sub-microsecond time scale, because of the small volume of the hot-spot. The estimated diffusion time would be 0.22 μs for an Atto-655 molecule diffusing in water across the transverse dimension of 10 nm calculated for the near field in the gap region. The retrieved relaxation time of 20 μs could be tentatively explained by transient sticking of the dye to DNA linkers, or simply, by the limited time resolution of our correlation curves that allows us only to measure a relaxation tail of the fast decay component. On the other hand, the long decay component occurs on a similar time scale for the correlation function of enhanced and non-enhanced emission (inset

of Fig. 6D). The average relaxation time of this long component is around 2.7 ms, and is attributed to the dye's adsorption/desorption on the surface surrounding the dimer particle. A similar behavior has been previously reported for emission enhancement of single-molecule fluorescence using surface immobilized gold nanorods.[19,28] The slower motion of dye molecules due to sticking onto the surface, or even due to interaction with DNA linkers, seems to be corroborated by intense emission events that last longer than a few ms, which are seldom observed in emission traces (Fig. S8 of the SI). Alternatively, it is possible to retrieve separate correlation functions for enhanced and non-enhanced emission by using the polarization properties of the longitudinal surface plasmon mode.[21] Here, we have used the emission polarization of dimer particles to select those that are aligned in such a way that emission along the LSP mode, or perpendicular to it, was divided by the beam-splitter analyzer into two detection channels (Fig. S9 of the SI). The correlation function of the enhanced emission shows at short times an additional relaxation component that is not present in correlation of non-enhanced emission, similarly to the FLCS analysis. The comparable results between these approaches validate the use of FLCS to separate enhanced from non-enhanced emission in plasmon-coupled fluorescence, as shown here.

Conclusions

We have confirmed that gold nanoparticle dimers produced by DNA self-assembly make efficient plasmonic antennas for fluorescence enhancement of red-emitting dyes. The combination of large-sized nanoparticles with nanometric gaps generate hot-spots with intense near fields in the interparticle region that are able to enhance the fluorescence of Atto-655 dye by

more than 1000-fold, while in some cases, top emission enhancements reach almost 4000-fold. Fluorescence lifetime correlation lead to the recovery of a short relaxation component exclusive to the enhanced emission likely due to the dye interaction with DNA linkers. The DNA-directed assembly approach used here allows for control over the association of dimer particles that is not possible with spontaneous particle aggregation, and is considerably more simple and affordable than approaches based on DNA origami templates. These two features of dimer particles, i.e. large fluorescence enhancements and preparation by affordable self-assembly colloidal methods, renders these plasmonic antennas promising for application in optical imaging or sensing. We have also shown that fluorescence lifetime correlation spectroscopy can be used to separate plasmon-enhanced from non-enhanced emission. Further studies using this approach will enable to explore its potential in extracting more information from plasmon-enhanced fluorescence.

ASSOCIATED CONTENT

Supporting Information. Oligonucleotide sequences of DNA linkers; Additional images of purification gels, optical microscopy and TEM of dimer particle samples; Average emission intensity of non-enhanced Atto-655 dye; Analysis of number and duration of fluorescence bursts; Fluorescence decays of Atto-655 enhanced and non-enhanced emission; Additional FLCS analysis and examples of time traces showing long events of enhanced emission; FCS analysis of polarization resolved emissions; Details on the estimation of fluorescence enhancement from DDA calculations.

The following files are available free of charge.

brief description (file type, i.e., PDF)

AUTHOR INFORMATION

Corresponding Author

* E-mail: pedro.m.paulo@tecnico.ulisboa.pt

Author Contributions

The manuscript was written through contributions of all authors. All authors have given approval to the final version of the manuscript.

Funding Sources

Fundação para a Ciência e a Tecnologia, FCT.

ACKNOWLEDGMENT

Authors gratefully acknowledge financial support from Fundação para a Ciência e a Tecnologia, FCT (REEQ/115/QUI/2005, Pest-OE/QUI/UI0100/2013/2014, UID/BIO/04565/2013 and PTDC/CTM-NAN/2700/2012). PMRP acknowledges a Post-Doc grant from FCT (SFRH/BPD/111906/2015). DB acknowledges a PhD grant from BIOTECnico Program (PD/BD/113630/2015).

REFERENCES

1 Giannini, V.; Fernández-Domínguez, A. I.; Heck, S. C.; Maier, S. A. Plasmonic Nanoantennas: Fundamentals and Their Use in Controlling the Radiative Properties of Nanoemitters. *Chem. Rev.* **2011**, *111*, 3888-3912.

2 Novotny, L.; van Hulst, N. Antennas for Light. *Nat. Photon.* **2011**, *5*, 83-90.

3 Biagioni, P.; Huang, J.-S.; Hecht, B. Nanoantennas for Visible and Infrared Radiation. *Rep. Prog. Phys.* **2012**, *75*, 024402-40.

4 Anger, P.; Bharadwaj, P.; Novotny, L. Enhancement and Quenching of Single-Molecule Fluorescence. *Phys. Rev. Lett.* **2006**, *96*, 113002-4.

5 Kühn, S.; Håkanson, U.; Rogobete, L.; Sandoghdar, V. Enhancement of Single-Molecule Fluorescence Using a Gold Nanoparticle as an Optical Nanoantenna. *Phys. Rev. Lett.* **2006**, *97*, 017402-4.

6 Kinkhabwala, A.; Yu, Z.; Fan, S.; Avlasevich, Y.; Müllen, K.; Moerner, W. E. Large Single-Molecule Fluorescence Enhancements Produced by a Bowtie Nanoantenna. *Nat. Photon.* **2009**, *3*, 654−657.

7 Yuan, H.; Khatua, S.; Zijlstra, P.; Yorulmaz, M.; Orrit, M. Thousand-fold Enhancement of Single-Molecule Fluorescence Near a Single Gold Nanorod. *Angew. Chem., Int. Ed.* **2013**, *52*, 1217−1221.

8 Muskens, O. L.; Giannini, V.; Sánchez-Gil, J. A.; Rivas, J. G. Strong Enhancement of the Radiative Decay Rate of Emitters by Single Plasmonic Nanoantennas. *Nano Lett.* **2007**, *7*, 2871-2875.

9 Ringler, M.; Schwemer, A.; Wunderlich, M.; Nichtl, A.; Kürzinger, K.; Klar, T. A.; Feldmann, J. Shaping Emission Spectra of Fluorescent Molecules with Single Plasmonic Nanoresonators. *Phys. Rev. Lett.* **2008**, *100*, 203002-4.

10 Busson, M. P.; Rolly, B.; Stout, B.; Bonod, N.; Bidault, S. Accelerated Single Photon Emission from Dye Molecule-Driven Nanoantennas Assembled on DNA. *Nat. Commun.* **2012**, *3*, 962−966.

11 Li, J.; Krasavin, A. V.; Webster, L.; Segovia, P.; Zayats, A. V.; Richards, D. Spectral Variation of Fluorescence Lifetime Near Single Metal Nanoparticles. *Sci Rep.* **2016**, *6*, 21349-9.

12 Kosako, T.; Kadoya, Y.; Hofmann, H. F. Directional Control of Light by a Nano-Optical Yagi–Uda Antenna. *Nat. Photon.* **2010**, *4*, 312-315.

13 Curto, A. G.; Volpe, G.; Taminiau, T. H.; Kreuzer, M. P.; Quidant, R.; van Hulst, N. F. Unidirectional Emission of a Quantum Dot Coupled to a Nanoantenna. *Science* **2010**, *329*, 930-933.

14 Jain, P. K.; Ghosh, D.; Baer, R.; Rabani, E.; Alivisatos, A. P. Near-Field Manipulation of Spectroscopic Selection Rules on the Nanoscale. *Proc. Natl. Acad. Sci.* **2012**, *109*, 8016-8019.

15 Ueno, K.; Juodkazis, S.; Shibuya, T.; Yokota, Y.; Mizeikis, V.; Sasaki, K.; Misawa, H. Nanoparticle Plasmon-Assisted Two-Photon Polymerization Induced by Incoherent Excitation Source. *J. Am. Chem. Soc.* **2008**, *130*, 6928-6929.

16 de Torres, J.; Mivelle, M.; Moparthi, S. B.; Rigneault, H.; Van Hulst, N. F.; García-Parajó, M. F.; Margeat, E.; Wenger, J. Plasmonic Nanoantennas Enable Forbidden Förster Dipole−Dipole Energy Transfer and Enhance the FRET Efficiency. *Nano Lett.* **2016**, *16*, 6222-6230.

17 Pellegrotti, J. V.; Acuna, G. P.; Puchkova, A.; Holzmeister, P.; Gietl, A.; Lalkens, B.; Stefani, F. D.; Tinnefeld, P. Controlled Reduction of Photobleaching in DNA Origami-Gold Nanoparticle Hybrids. *Nano Lett.* **2014**, *14*, 2831-2836.

18 Warren, S. C.; Thimsen, E. Plasmonic Solar Water Splitting. *Energy Environ. Sci.* **2012**, *5*, 5133-5146.

19 Khatua, S.; Yuan, H.; Orrit, M. Enhanced-Fluorescence Correlation Spectroscopy at Micro-molar Dye Concentration around a Single Gold Nanorod. *Phys. Chem. Chem. Phys*. **2015**, *17*, 21127-21132.

20 Pradhan, B.; Khatua, S.; Gupta, A.; Aartsma, T.; Canters, G.; Orrit, M. Gold-Nanorod-Enhanced Fluorescence Correlation Spectroscopy of Fluorophores with High Quantum Yield in Lipid Bilayers. *J. Phys. Chem. C* **2016**, *120*, 25996-26003.

21 Punj, D.; Regmi, R.; Devilez, A.; Plauchu, R.; Moparthi, S. B.; Stout, B.; Bonod, N.; Rigneault, H.; Wenger, J. Self-Assembled Nanoparticle Dimer Antennas for Plasmonic-Enhanced Single-Molecule Fluorescence Detection at Micromolar Concentrations. *ACS Photonics* **2015**, *2*, 1099-1107.

22 Cang, H.; Labno, A.; Lu, C.; Yin, X.; Liu, M.; Gladden, C.; Liu, Y.; Zhang, X. Probing the Electromagnetic Field of a 15-nanometre Hotspot by Single Molecule Imaging. *Nature* **2011**, *469*, 385-388.

23 Wertz, E.; Isaacoff, B. P.; Flynn, J. D.; Biteen, J. S. Single-Molecule Super-Resolution Microscopy Reveals How Light Couples to a Plasmonic Nanoantenna on the Nanometer Scale. *Nano Lett.* **2015**, *15*, 2662-2670.

24 Su, L.; Yuan, H.; Lu, G.; Rocha, S.; Orrit, M.; Hofkens, J.; Uji-i, H. Super-resolution Localization and Defocused Fluorescence Microscopy on Resonantly Coupled Single-Molecule, Single-Nanorod Hybrids. *ACS Nano* **2016**, *10*, 2455-2466.

25 Taminiau, T. H.; Stefani, F. D.; van Hulst, N. F. Single Emitters Coupled to Plasmonic Nano-Antennas: Angular Emission and Collection Efficiency. *New J. Phys.* **2008**, *10*, 105005-16.

26 Rogobete, L.; Kaminski, F.; Agio, M.; Sandoghdar, V. Design of Plasmonic Nanoantennae for Enhancing Spontaneous Emission. *Opt. Lett.* **2007**, *32*, 1623-1625.

27 Bharadwaj, P.; Novotny, L. Spectral Dependence of Single Molecule Fluorescence Enhancement. *Opt. Express* **2007**, *15*, 14266-14274.

28 Khatua, S.; Paulo, P. M.; Yuan, H.; Gupta, A.; Zijlstra, P.; Orrit, M. Resonant Plasmonic Enhancement of Single-Molecule Fluorescence by Individual Gold Nanorods. *ACS Nano* **2014**, *8*, 4440-4449.

29 Wientjes, E.; Renger, J.; Cogdell, R.; van Hulst, N. F. Pushing the Photon Limit: Nanoantennas Increase Maximal Photon Stream and Total Photon Number. *J. Phys. Chem. Lett.* **2016**, *7*, 1604-1609.

30 Acuna, G. P.; Möller, F. M.; Holzmeister, P.; Beater, S.; Lalkens, B.; Tinnefeld, P. Fluorescence Enhancement at Docking Sites of DNA Directed Self-Assembled Nanoantennas. *Science* **2012**, *338*, 506-510.

31 Bidault, S.; Devilez, A.; Maillard, V.; Lermusiaux, L.; Guigner, J.-M.; Bonod, N.; Wenger J. Picosecond Lifetimes with High Quantum Yields from Single-Photon Emitting Colloidal Nanostructures at Room Temperature. *ACS Nano* **2016**, *10*, 4806-4815.

32 Zhang, T.; Gao, N.; Li, S.; Lang, M. J.; Xu Q.-H. Single-Particle Spectroscopic Study on Fluorescence Enhancement by Plasmon Coupled Gold Nanorod Dimers Assembled on DNA Origami. *J. Phys. Chem. Lett.* **2015**, *6*, 2043-2049.

33 Puchkova, A.; Vietz, C.; Pibiri, E.; Wünsch, B.; Paz, M. S.; Acuna, G. P.; Tinnefeld, P. DNA Origami Nanoantennas with over 5000-fold Fluorescence Enhancement and Single-Molecule Detection at 25 μM. *Nano Lett.* **2015**, *15*, 8354-8359.

34 Flauraud, V.; Regmi, R.; Winkler, P. M.; Alexander, D. T. L.; Rigneault, H.; van Hulst, N. F.; Garcia-Parajo, M. F.; Wenger, J.; Brugger, J. In-plane plasmonic antenna arrays with surface nanogaps for giant fluorescence enhancement. *Nano Lett.* **2017**, *17*, 1703-1710.

35 Teixeira, R.; Paulo, P. M. R.; Costa, S. M. B. Gold Nanoparticles in Core−Polyelectrolyte−Shell Assemblies Promote Large Enhancements of Phthalocyanine Fluorescence. *J. Phys. Chem. C* **2015**, *119*, 21612-21619.

36 Lan, X.; Chen, Z.; Liu, B.-J.; Ren, B.; Henzie, J.; Wang, Q. DNA-Directed Gold Nanodimers with Tunable Sizes and Interparticle Distances and Their Surface Plasmonic Properties. *Small* **2013**, *9*, 2308-2315.

37 Paulo, P. M. R.; Costa, S. M. B. Single-Molecule Fluorescence of a Phthalocyanine in PAMAM Dendrimers Reveals Intensity−Lifetime Fluctuations from Quenching Dynamics. *J. Phys. Chem. C* **2010**, *114*, 19035-19043.

38 Gregor, I.; Enderlein, J. Time-resolved Methods in Biophysics. 3. Fluorescence Lifetime Correlation Spectroscopy. *Photochem. Photobiol. Sci.* **2007**, *6*, 13-18.

39 Kapusta, P.; Macháň, R.; Benda, A.; Hof, M. Fluorescence Lifetime Correlation Spectroscopy (FLCS): Concepts, Applications and Outlook. *Int. J. Mol. Sci.* **2012**, *13*, 12890-12910.

40 Hill, H. D.; Millstone, J. E.; Banholzer, M. J.; Mirkin, C. A. The Role Radius of Curvature Plays in Thiolated Oligonucleotide Loading on Gold Nanoparticles. *ACS Nano* **2009**, *3*, 418-424.

41 Zhang, X.; Gouriye, T.; Göeken, K.; Servos, M. R.; Gill, R.; Liu, J. Toward Fast and Quantitative Modification of Large Gold Nanoparticles by Thiolated DNA: Scaling of

Nanoscale Forces, Kinetics, and the Need for Thiol Reduction. *J. Phys. Chem. C* **2013**, *117*, 15677−15684.

42 Teixeira, R.; Paulo, P. M. R.; Viana, A. S.; Costa, S. M. B. Plasmon-Enhanced Emission of a Phthalocyanine in Polyelectrolyte Films Induced by Gold Nanoparticles. *J. Phys. Chem. C* **2011**, *115*, 24674–24680.

43 Yurkin, M. A.; Hoekstra, A. G. The Discrete-Dipole-Approximation Code ADDA: Capabilities and Known Limitations. *J. Quant. Spectrosc. Radiat. Transfer* **2011**, *112*, 2234-2247.

44 Johnson, P. B.; Christy, R. W. Optical Constants of Noble Metals. *Phys. Rev. B* **1972**, *6*, 4370-4379.

45 D'Agostino, S.; Pompa, P. P.; Chiuri, R.; Phaneuf, R.; Britti, D. G.; Rinaldi, R.; Cingolani, R.; Della Sala, F. Enhanced Fluorescence by Metal Nanospheres on Metal Substrates. *Opt. Lett.* **2009**, *34*, 2381-2383.

46 D'Agostino, S.; Della Sala, F.; Andreani, L. C. Dipole-Excited Surface Plasmons in MetallicNanoparticles: Engineering Decay Dynamics within the Discrete-DipoleApproximation. *Phys. Rev. B: Condens. Matter Mater. Phys.* **2013**, *87*, 205413−13.

47 Nordlander, P.; Oubre, C.; Prodan, E.; Li, K.; Stockman, M. I. Plasmon Hybridization in Nanoparticle Dimers. *Nano Lett.* **2004**, *4*, 899-903.